

MIT Open Access Articles

CO₂ emissions from an undrained tropical peatland: Interacting influences of temperature, shading and water table depth

The MIT Faculty has made this article openly available. **Please share** how this access benefits you. Your story matters.

Citation: Hoyt, Alison M., Gandois, Laure, Eri, Jangarun, Kai, Fuu Ming, Harvey, Charles F. et al. 2019. "CO₂ emissions from an undrained tropical peatland: Interacting influences of temperature, shading and water table depth." *Global Change Biology*, 25 (9).

As Published: <http://dx.doi.org/10.1111/gcb.14702>

Publisher: Wiley

Persistent URL: <https://hdl.handle.net/1721.1/141006>

Version: Author's final manuscript: final author's manuscript post peer review, without publisher's formatting or copy editing

Terms of use: Creative Commons Attribution-Noncommercial-Share Alike



1

2 DR. ALISON HOYT (Orcid ID : 0000-0003-0813-5084)

3 DR. ALEXANDER R COBB (Orcid ID : 0000-0002-3128-3002)

4

5

6 Article type : Primary Research Articles

7

8

9 Corresponding Author Email ID: ahoyt@mit.edu

10 **CO₂ emissions from an undrained tropical peatland: Interacting influences of**
11 **temperature, shading and water table depth**

12

13 Alison M. Hoyt^{1,a}, Laure Gandois², Jangarun Eri^{3,c}, Fuu Ming Kai^{4,b}, Charles F. Harvey^{1,4,d},
14 Alexander R. Cobb^{4,d}

15

16 ¹ Department of Civil and Environmental Engineering, Massachusetts Institute of Technology, Cambridge,
17 Massachusetts, 02139 USA

18 ² EcoLab (Laboratoire Écologie fonctionnelle et Environnement), Université de Toulouse, CNRS, INPT, UPS,
19 Toulouse, France

20 ³ Forestry Department, Ministry of Industry and Primary Resources, Jalan Menteri Besar, Bandar Seri Begawan
21 BB3910, Brunei Darussalam

22 ⁴ Center for Environmental Sensing and Modeling, Singapore-MIT Alliance for Research and Technology, 138602
23 Singapore

24 ^a Present address: Max Planck Institute for Biogeochemistry, 07745 Jena Germany

25 ^b Present address: Gas Metrology Laboratory, National Metrology Center, Agency for Science, Technology and
26 Research, 118221 Singapore

This is the author manuscript accepted for publication and has undergone full peer review but has not been through the copyediting, typesetting, pagination and proofreading process, which may lead to differences between this version and the [Version of Record](#). Please cite this article as [doi: 10.1111/GCB.14702](https://doi.org/10.1111/GCB.14702)

This article is protected by copyright. All rights reserved

27 ^c Present address: Forestry Department, Ministry of Primary Resources and Tourism, Jalan Menteri Besar, Bandar
28 Seri Begawan BB3910, Brunei Darussalam

29 ^d C.F.H. and A.R.C. should be considered joint senior author

30

31

32 **Abstract**

33

34 Emission of CO₂ from tropical peatlands is an important component of the global carbon budget.
35 Over days to months, these fluxes are largely controlled by water table depth. However, the diurnal cycle
36 is less well understood, in part, because most measurements have been collected daily at midday. We
37 used an automated chamber system to make hourly measurements of peat surface CO₂ emissions from
38 chambers root-cut to 30cm. We then used these data to disentangle the relationship between temperature,
39 water table, and heterotrophic respiration (R_{het}). We made two central observations. First, we found strong
40 diurnal cycles in CO₂ flux and near-surface peat temperature (<10 cm depth), both peaking at midday.
41 The magnitude of diurnal oscillations was strongly influenced by shading and water table depth,
42 highlighting the limitations of relying on daytime measurements and/or a single correction factor to
43 remove daytime bias in flux measurements. Second, we found mean daily R_{het} had a strong linear relation
44 to the depth of the water table and under flooded conditions, R_{het} was small and constant. We used this
45 relationship between R_{het} and water table depth to estimate carbon export from both R_{het} and DOC over
46 the course of a year based on water table records. R_{het} dominates annual carbon export, demonstrating the
47 potential for peatland drainage to increase regional CO₂ emissions. Finally, we discuss an apparent
48 incompatibility between hourly and daily-average observations of CO₂ flux, water table and temperature:
49 water table and daily average flux data suggest that CO₂ is produced across the entire unsaturated peat
50 profile, whereas temperature and hourly flux data appear to suggest that CO₂ fluxes are controlled by very
51 near surface peat. We explore how temperature, moisture, and gas transport related mechanisms could
52 cause mean CO₂ emissions to increase linearly with water table depth but also have a large diurnal cycle.

53

54 *Keywords:* heterotrophic respiration, CO₂ flux, diurnal cycle, soil temperature, closed dynamic
55 chamber technique, tropical peatland, Southeast Asia

56

57 **Introduction**

58 There are 24.8 Mha of tropical peatlands in Southeast Asia that sequester 68.5 GtC
59 (gigatons of carbon; Page *et al.*, 2011a). Existing peat deposits in Southeast Asia began to

60 accumulate around 15 ka (kiloannum BP), and expanded rapidly in coastal areas following the
61 last sea level highstand at about 4.5 ka (Dommain *et al.*, 2014). Across Southeast Asia, this large
62 store of carbon is being released to the atmosphere as CO₂ as peatlands are deforested and
63 drained (Hooijer *et al.*, 2010). Conversion and deforestation rates are high, and in 2015, only
64 6.4% of the 15.7 Mha of peatlands in Sumatra, Borneo and Peninsular Malaysia remained as
65 pristine peat swamp forest (Miettinen *et al.*, 2016).

66
67 Drainage of peatlands releases sequestered carbon to the atmosphere. In natural
68 peatlands, peat soil accumulates under waterlogged conditions as the rate of plant productivity
69 exceeds the rate of decomposition due to a lack of oxygen available for decomposition. When the
70 water table is lowered, either seasonally or through drainage projects, oxygen becomes available
71 for aerobic decomposition of organic matter. The resulting release of CO₂ to the atmosphere is
72 both a significant source of greenhouse gases, and is responsible for long-term subsidence of the
73 peat surface (Hooijer *et al.*, 2012). Emissions from peat oxidation excluding fires in 2015 were
74 estimated to range from 132-159 MtC/yr, and cumulative carbon emissions since 1990 are
75 estimated at 2.5 GtC (Miettinen *et al.*, 2017). The associated subsidence rates due to peat
76 oxidation in drained peatlands can remain as high as 5 cm/yr for decades following drainage
77 (Hooijer *et al.*, 2012). At these rates, many coastal peatland areas are in danger of subsiding
78 below sea level.

79
80 Both subsidence-based estimates of carbon loss and measurements of CO₂ efflux with
81 respiration chambers have found that peatland CO₂ emissions are strongly correlated with the
82 average water table depth on weekly to monthly timescales (reviewed in Couwenberg *et al.*,
83 2010; Carlson *et al.*, 2015). However, some natural and physical processes are likely to cause
84 changes in CO₂ fluxes on shorter timescales. Like other biological processes, decomposition is
85 affected by temperature, which varies diurnally (Davidson & Janssens, 2006). Circadian patterns
86 in assimilate transport to roots drive diurnal patterns in root exudation, which can create diurnal
87 pattern in soil CO₂ flux (reviewed in Kuzyakov, 2006). The correlation between emissions and
88 water table depth is clearly documented over longer timescales, but few studies have measured
89 emissions at sub-diurnal timescales in tropical peatlands due to logistical challenges. Despite the
90 clear long-term dependence of peat oxidation and the corresponding CO₂ efflux on water table

91 depth, the relationships between temperature, water table and CO₂ emissions on shorter
92 timescales remain unclear (Jauhiainen *et al.*, 2012).

93 Automated chambers have been used to capture CO₂ fluxes over the 24-hour cycle
94 (Hirano *et al.*, 2009, 2014; Ishikura *et al.*, 2018a) in only a few of the more than 20 studies
95 measuring CO₂ emissions from tropical peatlands in Southeast Asia. Instead, the majority of
96 studies rely on manual measurements, most often collected at midday (e.g. Melling *et al.*, 2005;
97 Jauhiainen *et al.*, 2014). Perhaps in part due to sparse datasets, efforts to characterize the diurnal
98 cycle and temperature dependence of CO₂ fluxes have found mixed results. Hirano *et al.* (2009)
99 found a clear midday peak in CO₂ emissions using automated chambers. Higher midday fluxes
100 were also detected in manual chamber measurements over more limited time periods (1 day –
101 two weeks) by Ali *et al.* (2006), Husnain *et al.* (2014), Marwanto & Agus (2014) and Comeau *et al.*
102 *al.* (2016). However, Hergoualc'h *et al.* (2017) did not detect a diurnal cycle in CO₂ flux, and
103 Ishikura *et al.* (2018) measured the lowest average hourly CO₂ fluxes at midday.

104
105 Levels of shading, precipitation and temperature are expected to change in the future as a
106 result of changing climate and land use, and will influence rates of heterotrophic respiration
107 (R_{het}) in tropical peatlands. Hourly measurements could yield valuable mechanistic insights
108 about how R_{het} will respond to such changes. Soil respiration across ecosystems depends strongly
109 on temperature (Lloyd & Taylor, 1994; Fang & Moncrieff, 2001; Davidson *et al.*, 2006; Tuomi
110 *et al.*, 2008). In tropical peatlands, CO₂ emissions have been found to depend on water table
111 depth, as well as temperature (Hirano *et al.*, 2009), shading (Jauhiainen *et al.*, 2014), and time of
112 day (Ishikura *et al.*, 2018a). These observations have different implications for the primary
113 mechanisms driving R_{het} , as well as the depth distribution of peat decomposition.

114
115 Here we use hourly measurements to explore the relationship between temperature, water
116 table, shading and the diurnal cycle of peat CO₂ efflux. We find: (A) a clear relationship between
117 daily mean R_{het} and water table depth, which enables accurate upscaling of soil respiration fluxes
118 throughout the year based on water table alone; and (B) a strong diurnal cycle in CO₂ flux and
119 peat-surface temperature, highlighting the bias that can result from use of daytime measurements
120 alone. Finally, through physical calculations, we explore several mechanisms that could result in

121 the daily mean flux increasing linearly with water table depth while also having a large diurnal
122 cycle.

123

124 **Methods**

125

126 **Measurement location, climate and land conversion history**

127 Measurements were made in an undrained former timber concession in the Belait district
128 of Brunei Darussalam, on the island of Borneo (Figure 1f; 114.362787°E, 4.405100°N; Site 1b
129 within the Damit dome, 3.4km from the edge of the peat dome, as described in Gandois *et al.*
130 (2013)). This site is an area of regenerating peatland that was logged by rail in 200 m x 200 m
131 blocks from 1972-2010 but was not drained, and has been described in Kobayashi (1999),
132 Gandois *et al.* (2013) and Gandois *et al.* (2014). Prior to logging, the site had a monodominant
133 *Shorea albida* canopy. However, all but a few remnant trees were removed during logging, and
134 the site now hosts mostly low-statured vegetation at varying stages of regeneration. Although the
135 site was not drained, its vegetation resembles that of drained and degraded peatlands of Central
136 Kalimantan (Blackham *et al.*, 2013; Ishikura *et al.*, 2018b): the tree species *Combretocarpus*
137 *rotundatus*, a liana (*Uncaria* sp.), and ferns (*Nephrolepis* sp.) are common at the site. Figs (*Ficus*
138 sp.) are locally abundant near the chamber site (Figure 1).

139

140 The woody peat at the site is highly organic, with a loss on ignition of 99% and percent
141 carbon of 51% (Gandois *et al.*, 2013). The peat characteristics are expected to be very similar to
142 those documented in the adjacent Mendaram peatland site, where the primarily fibric and humic
143 woody peat has a dry bulk density of 0.072 ± 0.02 g cm⁻³ in the top 3.5m of the peat profile
144 (Dommain *et al.*, 2015). The peat microtopography at the site is also similar to that at the
145 adjacent Mendaram peatland site as described by Cobb *et al.* (2017), with local depressions
146 separated by mounds created by the accumulation of organic matter around deadfall or the
147 buttresses of live or dead trees (Figure 1; Figure S4).

148

149 Average precipitation measured at nearby Seria and Kuala Belait weather stations in
150 1947-2004 was 2880 mm/yr. The site is relatively aseasonal. Average precipitation was 139 mm

151 in the driest month (March) over the same interval, well above the threshold of 60 mm/mo for a
152 tropical dry season in the Köppen climate classification (Kottek *et al.*, 2006).

153

154 **Flux Measurements**

155 We used automated soil respiration chambers to measure fluxes of CO₂ from the peat
156 surface. Measurements were taken hourly at four chambers using an automated chamber system
157 (LI-8100 with LI-8150 multiplexer; LI-COR Biosciences). Opaque white chambers were 20cm
158 in diameter and had a volume of 4076.1 cm³. We measured fluxes from July – November 2012,
159 in both dry and flooded conditions (measurements in two chambers 7/13/12-8/5/12; four
160 chambers active from 8/7/12-11/23/12). The first chamber was located in a relatively open area,
161 with ferns and low-lying regenerating vegetation, and received direct sunlight during the day.
162 Three additional chambers were fully shaded, located beneath low tree canopy. All chambers
163 were installed at low points within the variable peat topography, and none were located directly
164 adjacent to trees, due to the practical consideration that cutting roots and anchoring collars
165 immediately adjacent to trees, or in higher topographic positions, where thick woody roots
166 dominate, was not feasible. The chambers were placed approximately 8 m apart along a north-
167 south transect (Figure 1e).

168

169 All chambers were mounted on tall collars (approx. 30cm tall). These collars significantly
170 increased the total measurement air volume, to 18688.1, 17258.0, 16781.3 and 19005.9 cm³
171 respectively for the four chambers. While this could reduce mixing within the collar, it was
172 necessary to avoid flooding of chamber electronics at the high water tables experienced at the
173 site. Each chamber was anchored into the peat using four legs constructed from 1m lengths of 2”
174 PVC pipe (Figure 1a-d).

175

176 Soil collars were installed in March 2012, four months prior to CO₂ flux measurements.
177 This long waiting period was designed to ensure any spike in respiration from the input of fresh
178 root material would have dissipated by the time measurements began. In tropical peatlands, a
179 substantial component of the peat mass is composed of dead root material, and very high rates of
180 root turnover have been documented (Brady, 1997; Wright *et al.*, 2011). As a result, it is likely
181 that after four months, labile root material had fully decomposed, leaving behind root remnants

182 similar to those found within the existing peat matrix. Collars were constructed from 8" grey
183 PVC pipe and were inserted to 30cm depth, the anticipated maximum depth of the water table,
184 after cutting a slot for the pipe into the peat with a straight hoe, and severing roots. Although the
185 water table dropped to 36cm below the peat surface during the study period, the time the water
186 table spent below the 30cm trenching depth was a small fraction of the study period (Figure 1).
187 Although we cannot rule out a small contribution from root respiration, from roots below 30cm,
188 or those which may have grown up into the chamber over the course of the study, we expect the
189 CO₂ fluxes measured are dominated by, and representative of, heterotrophic respiration.

190

191 Flux Calculations

192 Soil CO₂ fluxes from the peat surface, F , were calculated from the rate of change dC/dt in
193 the water-vapor corrected CO₂ mole fraction multiplied by the moles of dry gas n in the chamber
194 loop, divided by the soil surface area S , according to:

$$195 \quad F = \frac{ndC}{S dt} = \frac{10VP\left(1 - \frac{W}{1000}\right)dC}{RS(T + 273.15) dt} \quad [1]$$

196 where the CO₂ flux from the peat surface, F ($\mu\text{mol m}^{-2} \text{s}^{-1}$), depends on the total chamber volume
197 adjusted for water table depth, V (cm^3), the pressure, P (kPa), the water vapor mole fraction, W
198 (mmol mol^{-1}), the air temperature, T ($^{\circ}\text{C}$), the soil surface area, S (cm^2) and the rate of change in
199 the water-corrected CO₂ mole fraction, dC/dt ($\mu\text{mol mol}^{-1}$). dC/dt is calculated from the increase
200 in CO₂ concentration during chamber closure (LI-8150 manual, LI-COR, 2010). We obtained the
201 chamber air temperature from the built-in temperature sensor of a barometric pressure logger
202 (Barologger Gold, Solinst Canada Ltd.) suspended inside the collar of one of the shaded soil
203 chambers because of failure of the built-in chamber air temperature thermistors. The radiation
204 balance and thermal mass of the barometric pressure logger could result in slightly higher
205 estimates of chamber air temperature during the day and lower temperatures at night than the
206 built-in thermistors, and the volume of the logger slightly reduced the volume of the
207 measurement loop (<1.5%). Although air temperature measurements for flux calculations were
208 only made in a shaded chamber, uncertainty associated with the temperature in the sunny
209 chamber had a negligible impact on the fluxes (approximately 1.7% change in fluxes for
210 expected possible air temperature difference of 5 $^{\circ}\text{C}$, or up to 3.3% for 10 $^{\circ}\text{C}$). The fluxes reported

211 here correct those reported in Cobb *et al.* (2017) which used data from the faulty temperature
212 sensors, leading to a relative correction of approximately 20% greater fluxes.

213
214 Each flux measurement was made over a 6 minute chamber closure time. Chambers
215 rested open during the remaining period between hourly measurements (54 minutes). Throughout
216 the study period, and across chambers, we observed increases in the water vapor-corrected CO₂
217 mole fraction which showed no evidence of saturation, possibly because of the large total
218 chamber and collar volume or short closure time (Livingston *et al.*, 2005; Kutzbach *et al.*, 2007;
219 Heinemeyer & McNamara, 2011). Therefore, we calculated rates of change in water vapor-
220 corrected CO₂ mole fraction (dC/dt) from a linear fit to the data from 45s to 359s. An example
221 time series is shown in Figure S3. As a result of the highly linear data, only a negligible fraction
222 of data had fits with an $R^2 < 0.95$. Fluxes calculated from these fits were excluded from further
223 analysis (0.54% and 1.45% of data in July-Aug period; 1.15%, 0%, 0% and 0.08% of data in
224 Aug-Nov period for four chambers respectively). Instrument failure in October resulted in a
225 shorter time series for Chamber 2.

226

227 **Water table and Temperature measurements**

228 Throughout the CO₂ flux study period (July to November, 2012) we also measured the
229 water table depth, groundwater temperature (Levellogger Gold; Solinst Canada Ltd.; sensor
230 continually submerged at depth >35cm) and air temperature (Barologger Gold, Solinst Canada
231 Ltd.) adjacent to or within the shaded chamber (Period 1; Table 1). Additional water table
232 measurements were also made 4.1 km from our chamber measurement site at an adjacent pristine
233 peatland (the Mendaram peatland) described in Gandois *et al.* (2013), Dommmain *et al.* (2015) and
234 Cobb *et al.* (2017) and were used for upscaling (Figure 3) and to partition data period 2 into wet
235 and dry phases (Table 1; Figure S2) using a water table cutoff of 5cm below the peat surface.
236 Due to their proximity and the similar undrained nature of the sites, both sites experience similar
237 water table depths. The Mendaram water table time series was assembled from data from two
238 piezometers 130m apart (in and downslope of survey transect: Cobb *et al.*, 2017 Figure 2e). All
239 water table measurements, at both the Damit and Mendaram peatlands, were made relative to
240 low points, or hollows, in the peat surface. Peat soil temperature measurements were later made
241 at the peat surface, as well as 10cm and 25cm below the peat surface using TidbiT temperature

242 loggers (Onset, USA) from November 2013 to March 2014 (Period 2; Table 1) adjacent to both a
243 sunny and shaded chamber. Unfortunately concurrent measurements of peat CO₂ efflux and peat
244 temperature are not available, due to corrosion of the peat temperature sensor during Period 1.
245 However, these two measurement periods cover similar ranges of representative water table
246 depths, so qualitative comparisons are possible.

247

248 **Upscaling of Fluxes**

249 We modelled the fluxes of carbon leaving the peat dome throughout the year based on
250 their water table dependence and a time series of water table data. We used a linear fit to the flux
251 chamber daily mean data to model the heterotrophic peat surface CO₂ emission from local
252 depressions (hollows) similar to the sites of chamber installation. To estimate the overall flux
253 per area across the site, including higher areas in the microtopography, we assumed that higher
254 areas had a similar peat surface CO₂ emission vs. water table relationship to hollows, but that this
255 distribution was vertically shifted by the difference in peat surface height, based on similar
256 findings reported by Hirano et al (2009) for hummocks and hollows in Central Kalimantan.
257 Because the microtopography at the site resembles that of the adjacent Mendaram site, we used
258 the results of our earlier theodolite survey at that site (Cobb *et al.*, 2017) to obtain the average
259 height of the peat surface above the hollows for upscaling, by calculating the mean vertical offset
260 between the peat surface interpolated between survey points and a smooth reference surface fit
261 through local minima in the peat surface (Cobb *et al.*, 2017; Figure S4). We did not take the
262 fraction of shaded area into account when upscaling as mean daily CO₂ efflux was very similar
263 in the sunny and shaded chambers (Results).

264 We also estimated the total DOC export across different water table depths (Figure 3c) by
265 using the relationship between runoff and water table developed by Cobb (Equation 5 and “SI
266 Hydrologic Budget for Our Site” in Cobb *et al.*, 2017). We assumed this runoff carried a
267 constant average DOC concentration of 75mgC/L, based on repeated measurements of shallow
268 porewater at the site (Gandois *et al.*, 2013). We used three years of water table measurements
269 from the nearby and similarly undrained Mendaram peatland site, where a longer continuous
270 measurement time series was available. The data period from Feb 2012 – Feb 2015 included both
271 dry and wet conditions, capturing the end of La Niña in early 2012, and the beginning of El Niño
272 conditions in late 2014 and early 2015 (NOAA, 2019).

273

274 **Oxygen Diffusion Calculations**

275 We calculated the potential oxygen availability in the peat based on a diffusion equation.
276 The oxygen profile vs depth z is described by the 1-D diffusion equation with a constant
277 decomposition rate coefficient k :

$$278 \quad d \frac{d^2 C(z)}{dz^2} = -kC(z) \quad [2]$$

279 We assumed that oxygen consumption below the water table was negligible, which implies a
280 zero gradient boundary at the depth of the water table L and yields the solution:

$$281 \quad C(z) = C_0 \frac{\cosh\left[\sqrt{\frac{k}{d}}(L-z)\right]}{\cosh\left[\sqrt{\frac{k}{d}}L\right]} \quad [3]$$

282 where C_0 is the oxygen concentration in air (9.4 moles/m³) and d is the effective diffusion
283 coefficient of oxygen. We calculated a decomposition rate coefficient k [day⁻¹] for each day by
284 first solving for the diffusive flux $q = d \frac{dC}{dz}$ at the peat surface, $q = C_0 \sqrt{dk} \tanh\left[\sqrt{\frac{k}{d}}L\right]$, then
285 setting q equal to the measured average flux for the day, and solving for k assuming an effective
286 oxygen diffusion coefficient of 0.5 m²/day, the coefficient in air (1.5 m²/day) reduced by a
287 tortuosity of 3 (Cussler, 1997; Rezanezhad *et al.*, 2010; Gharedaghloo *et al.*, 2018). Because the
288 daily average flux q increased nearly linearly with water table depth L , the calculated value of k
289 remained relatively uniform over the study period. These k values were compared to
290 decomposition rates derived from incubation experiments (e.g. Jauhainen *et al.*, 2016) by
291 multiplying the rate of CO₂ production during the incubation by the dry bulk density of the peat.

292

293 **Results**

294

295 **Water table**

296 The study period (July-Nov 2012) included both wet and dry periods, capturing the full
297 range of typical conditions for this undrained site. Beginning with dry conditions in August, the
298 water table rose over the course of the measurements (Figure 2; Figure S1). Water table depth

299 ranged from 36cm below the peat surface to 20cm above the peat surface. This is representative
300 of conditions at the nearby pristine site (Mendaram); the water table rarely drops more than 20-
301 30 cm below the peat surface (Figure 3).

302

303 **Air and Soil Temperature**

304 Air temperatures ranged from 20.8-34.8°C over the period of chamber measurements
305 (Aug-Nov 2012), with a daily mean of $25.3 \pm 2.2^\circ\text{C}$. The daily range in air temperature was
306 dependent on the water table depth, with the largest diurnal fluctuations in temperature occurring
307 when the water table was lowest (Figure 4). As the water table rose, the diurnal temperature
308 range decreased (Figure 4h).

309

310 Temperatures measured at the peat surface followed a similar diurnal cycle. The daily
311 peaks in temperature were strongest under dry conditions. Measured temperature increases were
312 also larger in the sun than in the shaded chamber. The largest diurnal swings in peat surface
313 temperature recorded, 49°C at midday and 22°C overnight, were found at the sunny location
314 when the water table is low. At high water levels, temperature oscillations at the surface peat
315 were damped, but not delayed. At depth, soil temperature fluctuations were buffered and lagged
316 relative to the surface peat. Temperature fluctuations 10 cm and 25 cm below the peat surface
317 were small (Figure 4c-f).

318

319 However, despite these differences in the diurnal peat temperature, there was little change
320 in the mean daily air temperature over the study period (Figure 4h). Similarly, the mean peat
321 temperature measurements made during Period 2 (Nov 2013-Mar 2014; Figure S2) were
322 remarkably uniform across locations and depths, ranging between 24.9-25.1°C (Figure 4). High
323 peat temperatures during the day were offset by cooler temperatures at night so that the daily
324 average changed little from day to day even as oscillations increased in magnitude with the water
325 table depth. Daily mean peat temperatures were similar across depths and shading conditions.
326 Where diurnal temperature oscillations were largest (surface measurement of sunny chamber) the
327 daily mean peat temperature was $25.1 \pm 1.6^\circ\text{C}$. Where oscillations were negligible (25 cm below
328 surface, shaded chamber), the daily mean peat temperature was nearly constant at $24.9 \pm 0.7^\circ\text{C}$.

329 The mean groundwater temperature measured at the site is $25.0 \pm 0.4^\circ\text{C}$, essentially stable at the
330 annual mean (measured Mar 2014-Sept 2015).

331

332 **Peat surface CO₂ emission**

333 Daily mean fluxes ranged from 0.5-8 $\mu\text{mol}/\text{m}^2/\text{s}$ and closely followed trends in the water
334 table (Figure 2). When the water table was at, or above, the local peat surface, the CO₂ flux from
335 the peat or water surface was small, with a daily mean value of 0.4 $\mu\text{mol}/\text{m}^2/\text{s}$. The daily mean
336 flux increased when the water table fell below the local peat surface, growing to $\sim 6 \mu\text{mol}/\text{m}^2/\text{s}$
337 when the water table depth was 30 cm. The increase in daily mean flux when the water table was
338 below the surface was nearly linear ($R^2 = 0.92$; Figure 3). Fluxes were highest under dry
339 conditions in July and August and decreased over the measurement period (Figure S1).

340

341 Measured hourly CO₂ flux was variable and showed a strong diurnal pattern (Figure 2b,
342 2d, Figure 4), with maximum CO₂ fluxes observed at midday. The amplitude of the diurnal cycle
343 increased as the water table dropped. Under the driest conditions, this effect was strongest, and
344 CO₂ flux reached a clearly defined maximum at mid-day when the temperature was highest (with
345 daily maximums 120% and 276% of the daily mean in the shade and sun respectively for water
346 table depths $>30\text{cm}$; Figure 4a,b & Figure 5). In contrast, at higher water tables, the diurnal
347 oscillations in CO₂ flux became less pronounced (with daily maximums 106% (shade) and 134%
348 (sun) of the daily mean for water table depths of 5-20cm; Figure 4). Under flooded conditions
349 (water table $< 5 \text{ cm}$ below surface), fluxes were low and stable, and slightly lower during the day
350 than at night (Figure 5). This diurnal pattern was most pronounced in the sun chamber (Chamber
351 1; Figure 2 & 4). Less pronounced daily oscillations were observed in the shaded chambers
352 during dry periods (Chambers 2-4; Figure 2 & 4).

353

354 **Upscaling of Fluxes**

355 Over three years from Feb 2012- Feb 2015, the upscaled heterotrophic CO₂ emission
356 from our measurements of peat surface hollows was 20 $\text{MgCO}_2/\text{ha}/\text{yr}$, and our calculated CO₂
357 emission from R_{het} across the entire peat dome was 28 $\text{MgCO}_2/\text{ha}/\text{yr}$ (Figure 3), based on an
358 average height of peat above hollows of 4.8 cm (Figure S4). This value is a lower bound because
359 we calculate nearly zero flux when the water table is at the average height of 4.8cm or above, but

360 in fact there is still flux where the peat surface is higher than the average. Calculated carbon
361 export by DOC was 0.8 MgCO₂/ha/yr (Figure 3).

362

363

364

365 **Oxygen Diffusion Calculations**

366 Calculation using equation [3] shows that the oxygen concentration just above the water
367 table is reduced by 0.5% relative to oxygen at the peat surface when the water table is at a depth
368 of 30 cm. The calculated decomposition rate coefficient k yielding the mean daily surface fluxes
369 with this water table depth and uniform decomposition above the water table was $\sim 1.8 \times 10^{-5}$
370 $\mu\text{mol cm}^{-3} \text{ s}^{-1}$.

371

372 **Discussion**

373

374 We observed (A) a tight correlation between daily average R_{het} and water table depth, and
375 (B) strong diurnal oscillations in CO₂ flux and surface peat temperature. We first discuss the
376 relationship between daily average R_{het} and water table depth, and apply this relationship to
377 estimate carbon loss from the peat dome from water table records. We then explore the diurnal
378 oscillations in CO₂ flux and surface-peat temperature. In section (C) we attempt to reconcile the
379 underlying mechanisms responsible for these two key observations. Finally, we discuss the
380 limitations of our approach and the implications of our findings (sections D and E).

381

382 **A) Long-Term: Relation between Daily Average CO₂ Flux and Water Table Depth**

383

384 *(i) Heterotrophic respiration is proportional to water table depth*

385 We observe a nearly linear relationship between water table and daily average CO₂ flux
386 when the water level is below the peat surface, and small uniform fluxes when the peat is flooded
387 (Figure 2). This simple behavior agrees closely with the results of Hirano *et al.* (2009) in a non-
388 drained forest in southern Borneo, where seasonality in rainfall is stronger (Gastaldo, 2010). We
389 cannot test whether the flux plateaus to a nearly constant value after the water table falls deeper

390 than 30 cm, as shown in Hirano *et al.* (2009), because the water table at our undrained site rarely
391 fell below 30 cm during the study.

392
393 The simple empirical relation of R_{het} to water table depth provides a link between
394 hydrology and carbon dynamics that is useful in applications ranging from long-term models of
395 peat geomorphology, to prediction of peat surface subsidence, to upscaling of regional CO_2
396 emissions (next section). Cobb *et al.* (2017) used a linear relation of peat loss (and accumulation)
397 to water table depth to simulate the growth of peat domes over millennia. Although this model
398 includes input of new organic material from plants, the simple linear relation between
399 heterotrophic decomposition and water table described here is consistent with a linear net
400 accumulation model. Hooijer *et al.* (2010) used a similar relationship to forecast CO_2 emissions
401 from peatland drainage across Southeast Asia to 2100. Data compilations by Hooijer *et al.*
402 (2010) and Carlson *et al.* (2015) found that heterotrophic respiration and total carbon loss
403 increase linearly with falling water table in tropical peatlands drained for agriculture.

404
405 (ii) *Why is mean daily R_{het} so strongly correlated with water table depth?*

406 One simple explanation for the strong relationship between mean daily R_{het} and water
407 table depth is that a falling water table exposes additional peat to oxic conditions, which then
408 decomposes at a uniform daily average rate. This explanation requires that oxygen is available
409 throughout the unsaturated peat profile. We tested the plausibility of this assumption with a
410 simple calculation of the rate of oxygen diffusion into the peat (Methods). This calculation
411 shows that sufficient oxygen would be available to support decomposition anywhere above the
412 water table at all water table depths measured in this study (oxygen concentration reduced by
413 less than 0.5% with water table at 30 cm). Our calculations are robust because the only
414 adjustable parameter is the effective diffusion coefficient of CO_2 in soil gas, and it would have to
415 be more than an order of magnitude smaller to qualitatively change the conclusion. Additionally,
416 the calculated decomposition rate coefficient ($\sim 1.8 \times 10^{-5} \mu\text{mol cm}^{-3} \text{ s}^{-1}$) falls within the range of
417 values derived from tropical peat incubations by Jauhiainen *et al.*, 2016 (approximately 1×10^{-5} to
418 $4 \times 10^{-5} \mu\text{mol cm}^{-3} \text{ s}^{-1}$), and is broadly consistent with other incubation studies (Murayama &
419 Bakar, 1996a, 1996b). Although this result suggests there is sufficient oxygen to support uniform

420 decomposition throughout the peat profile, it does not provide an explanation for the daily
421 oscillations in CO₂ efflux. Other possible mechanisms are explored in Section C.

422 (iii) Upscaling CO₂ and DOC fluxes from timeseries of water table dynamics

423 The relation of R_{het} to water table facilitates temporal and spatial upscaling, because
424 water table depths are more easily monitored than is R_{het} over long time periods. Our calculations
425 of overall fluxes from R_{het} and DOC export showed that heterotrophic respiration from the peat
426 surface is the dominant mechanism for carbon export from the peat at low water table levels,
427 whereas DOC export increases in importance when the water table is high (Figure 3). At high
428 water levels, methane emissions from the peat surface may also play a role (Couwenberg *et al.*,
429 2010). Because water table dynamics are nearly uniform across the peat dome (Cobb et al, 2017),
430 these results upscale measurements of local water table dynamics to estimate carbon fluxes
431 across the entire dome.

432
433 At this site, the water table spends most of the time within 10 cm of the peat surface,
434 high enough that R_{het} is small, but low enough that runoff, and hence DOC exports, are also
435 small (histogram, Figure 3). Thus, the water table is most often at a depth that minimizes organic
436 carbon loss and favors peat accumulation. Other studies on a variety of land uses (secondary
437 forest, oil palm, other agriculture) have shown mostly higher annual CO₂ fluxes ranging from 26-
438 102 MgCO₂/ha/yr (reviewed in Page *et al.*, 2011b). Although for a given water table depth we
439 measure similar hourly fluxes to other studies, the total annual flux at our nondrained site (28
440 MgCO₂/ha/yr) is at the low end of this range due to the shallower average water table.

441

442

443

444 **B) Diurnal Cycles: Temperature and Heterotrophic CO₂ Flux**

445

446 (i) Diurnal cycle in temperature and CO₂ flux

447 Hourly measurements of air temperature, peat temperature, and CO₂ flux all followed a
448 very similar diurnal cycle (Figure 4). We observed strong temperature oscillations in the surface
449 peat, particularly in the sun and at low water tables. Deeper in the peat, temperature oscillations
450 were both damped and delayed relative to surface peat. These trends in peat temperature are

451 consistent with measurements by Jauhiainen *et al.* (2014), which also showed temperature
452 oscillations that were smaller and increasingly lagged with depth (oscillation amplitude of <1°C
453 at 30 cm and below).

454
455 The strong diurnal cycle in peat surface CO₂ flux closely mirrored trends in peat
456 temperature (Figure 4). The midday maximum in CO₂ flux coincided with the midday maximum
457 in air and peat surface temperatures. This peak in CO₂ flux was sharpest for the sunny chamber,
458 which also experienced the highest midday peat temperatures. Additionally, the largest
459 temperature oscillations, both in the air and in the peat, occurred under dry conditions, when the
460 largest diurnal peak in average CO₂ flux was also observed. This qualitative relationship suggests
461 the diurnal cycle in the peat CO₂ flux is primarily driven by changes in peat temperature.

462
463 The magnitude of the diurnal cycle of temperature and CO₂ flux was smaller in the
464 shaded chambers. This is consistent with shading experiments performed by Jauhiainen *et al.*
465 (2014), who found larger diurnal fluctuations in temperature and CO₂ flux at unshaded sites than
466 at shaded sites. Despite this large difference in daytime emissions, and in contrast to Jauhiainen
467 *et al.* (2014), we found no evidence that the mean daily heterotrophic CO₂ emissions were
468 different in the sun and shade (Figure 2) and observed very similar mean CO₂ flux values at each
469 chamber for a given water table depth.

470
471 *(ii) What drives the strong diurnal oscillations in CO₂ flux?*

472 The similarity between daily patterns of CO₂ flux and peat temperature suggests changes
473 in hourly CO₂ flux are driven by changes in peat temperature, either through direct or indirect
474 mechanisms. The simplest explanation is that a large fraction of decomposition occurs near the
475 surface and is driven by changes in the temperature of the shallow peat. Our data show that, for a
476 reasonable Q₁₀ value of less than 3 (Brady, 1997; Davidson *et al.*, 2006), only the very surface of
477 the peat could produce oscillations in R_{het} of the amplitude observed in the peat surface CO₂
478 efflux. The much smaller temperature oscillations measured at 10 cm depth cannot produce such
479 large oscillations in CO₂ production for any reasonable Q₁₀ value. Thus, temperature-dependent
480 decomposition can only fully explain daily flux oscillations if flux is dominated by
481 decomposition in near-surface peat. Other studies have observed similar diurnal temperature

482 fluctuations (Hirano *et al.*, 2009, 2014, Jauhiainen *et al.*, 2012, 2014). As a result of their
483 observations, Jauhiainen *et al.* (2012, 2014) suggested that peat oxidation was concentrated in
484 the upper 10cm of the peat profile, perhaps due to the higher concentrations of oxygen and labile
485 carbon available for heterotrophic decomposition. However, we note that it is more difficult to
486 explain the increase in CO₂ flux with depth of water table if decomposition is concentrated in the
487 surface peat. Other possible mechanisms are explored in Section C.

488

489 *(iii) Importance of hourly measurements*

490 This dataset highlights the need for measurements around the diurnal cycle to accurately
491 estimate daily mean CO₂ efflux. Our observations, and similar findings from other studies that
492 employed automated chambers (Hirano *et al.*, 2009, 2014; Ishikura *et al.*, 2018a), show that it is
493 very difficult to interpret CO₂ flux measurements taken only during part of the day because of
494 large diurnal oscillations. Due to resource limitations, most measurements of CO₂ fluxes from
495 tropical peatlands have been made with manual chambers, usually during daylight, and often at
496 midday. The large daytime fluxes we observed, up to 180% above the diurnal average (Figure 5),
497 would bias emissions estimates if measurements were made only during the day. These results
498 demonstrate the importance of considering the diurnal cycle in experimental design. Use of a
499 correction factor to compute mean fluxes from daytime measurements, as applied in Jauhiainen
500 *et al.*, 2012, may provide a practical alternative to automated measurements (Jauhiainen *et al.*,
501 2012). However, our results suggest that such factors will depend on the water level regime at
502 each site and will vary over time.

503

504 In particular, care should be taken when interpreting daytime flux measurements from
505 unshaded open, degraded or logged peatlands, where diurnal fluctuations in peat temperature and
506 CO₂ flux may be large (Figure 4; Jauhiainen *et al.*, 2014). The Damit peat dome studied here was
507 selectively logged and retains scattered forest cover and areas of shade. However, other degraded
508 peatlands may be totally open, or have more limited fern or shrub cover. Under these conditions,
509 a pronounced diurnal cycle could strongly bias measurements. For example, in this study,
510 midday measurements made at the sunny chamber at water table levels deeper than 20 cm are
511 twice the mean daily flux (Figure 5). In other cases, day-time measurements could also
512 underestimate CO₂ fluxes, as observed by Ishikura *et al.* (2018).

513

514 *(iv) Thermal buffering and longer-term temperature stability*

515 Despite the temperature oscillations we observed, the mean peat temperature over the
516 study period was remarkably uniform across locations and depths, not differing by more than
517 0.2°C (Figure 4). Higher temperatures in the day were balanced by lower temperatures at night.
518 Similarly, the mean air temperature ($25.3 \pm 2.2^\circ\text{C}$) and groundwater temperatures ($25.0 \pm 0.4^\circ\text{C}$)
519 were very stable. As a result of the uniformity of mean daily temperature, temperature explained
520 little of the variability in mean daily R_{het} , which was driven instead by the level of the water table
521 (Figure 2).

522

523 Stable temperatures are maintained in large part by the thermal capacity of the underlying
524 groundwater. When the water table is near the surface, the heat capacity of the groundwater
525 dampens diurnal temperature variations; when the water table is lower, surface temperature
526 oscillations increase. However, the diurnal average remains close to the groundwater
527 temperature.

528

529 The greater temperature oscillations at the open sunny site indicate the importance of
530 radiation. During the day, the peat surface is heated by direct sunlight to much higher
531 temperatures than the shady locations; at night the open canopy allows radiative cooling of the
532 peat surface, offsetting higher daytime temperatures by the lowest nighttime temperatures
533 recorded in our study. Lower cloud cover during drier periods could also contribute to the larger
534 temperature fluctuations observed when the water table was low, by increasing both radiative
535 heating during the day and radiative cooling at night.

536

537 **C) Water Table and Temperature: Towards a Mechanistic Understanding of CO₂ Flux**

538

539 We observed (A) a linear increase in CO₂ flux with water table depth below the peat
540 surface, and (B) a large diurnal oscillation in CO₂ flux, correlated with oscillation in peat surface
541 temperature. Other studies of tropical peatland CO₂ flux with chambers have shown the same
542 basic phenomena (e.g., Jauhiainen *et al.*, 2012, 2014; Hirano *et al.*, 2014). There is a simple
543 explanation for each observation (A, B), but these simple explanations are not compatible. The

544 widely-observed depth dependence of emissions on water table depth (A) invites the simple
545 explanation that decomposition occurs at the same rate throughout the aerobic part of the soil
546 profile above the water table. Diurnal swings in emissions accompanying fluctuations in surface
547 soil temperature (B) suggest a different simple model: that decomposition is concentrated in the
548 near-surface peat. In this simple model, the diurnal fluctuations in temperature in the near-
549 surface soil drive diurnal changes in decomposition rates because of the temperature dependence
550 of decomposition. Each observation falsifies the simplest model for the other, implying that other
551 mechanisms governing soil gas exchange need to be considered to understand peat
552 decomposition. If we picture decomposition as uniform through the aerobic zone (simple
553 explanation A), how can emissions be 280% of the mean at mid-day (Figure 5), though large
554 temperature fluctuations are limited to near-surface peat (Figure 4; observation B)? On the other
555 hand, if we believe that emissions are dominated by decomposition in the near-surface peat
556 (simple explanation B), why do average emissions continue to increase as the water table recedes
557 to greater depths (observation A)? Although similar observations have been made before, there
558 has not been a systematic effort to reconcile the conflicting implications of these statements.

560 In this section we explore three mechanisms that could help answer these questions and
561 explain both observations A and B (Figure 6). First (i), we explore the possibility that the
562 increase in temperature oscillations at deeper water tables might promote more near-surface
563 decomposition. In this way, increasing water table depth would indirectly increase daily average
564 R_{het} . Second (ii), soil moisture could play a role in enhancing near-surface decomposition as the
565 water table drops. For example, as the water table falls, the aerobic peat above the water table
566 dries out, which could increase the rate of decomposition per volume of exposed peat. Finally
567 (iii), it is also possible that the daily oscillations in CO_2 flux reflect daily shifts in physical
568 transport processes that drive CO_2 out of the surface, rather than changes in decomposition rates.
569 Determining the roles of these mechanisms would provide insight into the physical and
570 biological mechanisms that control R_{het} , and could improve predictions of peat decomposition
571 under different temperature and water conditions.

572

573 *(i) Oscillating temperatures drive higher R_{het} because of nonlinearity*

574 The effect of temperature on respiration is typically represented using the Q_{10}
575 formulation. Because the Q_{10} formulation is nonlinear and convex, a greater range in
576 temperature, even at the same daily mean, could lead to a greater mean daily respiration rate.
577 Could larger temperature oscillations at low water tables drive both larger oscillations in fluxes
578 and larger daily mean fluxes from near-surface peat, explaining both observations A and B?

579 The ratio of the average decomposition rate over a day, $\overline{R(T(\tau))}$, to the decomposition
580 rate with the daily average temperature $R(\bar{T})$, is:

$$581 \quad \frac{\overline{R(T(\tau))}}{R(\bar{T})} = \frac{1}{24} \int_0^{24} Q_{10}^{(T(\tau) - \bar{T})/10} d\tau \quad [4]$$

582 where T is temperature, \bar{T} is the average temperature over the day, and τ is the hour of the day.
583 For the shady locations, where the oscillations span 24° to 30° with a mean of 25° , and with Q_{10}
584 set to 3 as an upper bound, equation [4] indicates an increase in mean daily flux of 10% caused
585 by oscillations, compared to the flux without oscillations. However, we observed a mean daily
586 flux about 10 times greater when the water table was at its lowest at both the sunny and shady
587 locations, indicating an increase in mean CO_2 flux of about 1000%. Therefore, nonlinear
588 dependence of decomposition on temperature alone cannot explain the strong increase in CO_2
589 flux as the water table falls with a reasonable value of Q_{10} .

590 (ii) Moisture controls on R_{het}

591 Soil heterotrophic respiration in unsaturated soil generally depends on both moisture and
592 temperature (Moyano *et al.* 2013). As the water table drops, soil moisture in the unsaturated zone
593 will also decrease. If this decrease in soil moisture causes a substantial increase in decomposition
594 of surface peat, this could explain both higher average fluxes at low water tables (A) and large
595 diurnal oscillations in fluxes (B).

596
597 Heterotrophic respiration is typically greatest at intermediate soil moisture, and lower at
598 very low and very high water contents (Moyano *et al.* 2013). Decomposition of near-surface peat
599 could begin to be reduced by desiccation at very low water tables (e.g. Hirano *et al.*, 2009;
600 Ishikura *et al.*, 2018), leading to a plateau in peat decomposition rates. In contrast, at wetter sites
601 like this one, surface peat decomposition could increase monotonically with drying over the

602 range of soil moisture contents. Experiments with a carbon-rich (60-70%) northern soil
603 (Wickland & Neff, 2008) show that microbial respiration increases by ~20% from saturated to
604 75% saturation. Moyano *et al.* (2013) describe a variety of mechanisms for increased respiration
605 with desaturation, including greater diffusion of oxygen in the gas phase and decreased predation
606 by microorganisms that can no longer find connected water pathways between soil aggregates.
607 To conclusively characterize this mechanism would require both detailed characterization of the
608 moisture profile above the water table and incubation experiments to characterize how moisture
609 content affects decomposition.

610

611 *(iii) Temperature-dependent transport processes*

612 An alternative mechanism that could help explain observations (A) and (B) is that daily
613 temperature oscillations could drive cycles in CO₂ transport. If diurnal oscillations in CO₂ fluxes
614 are partly accounted for by changes in transport of CO₂ out of the peat, decomposition could
615 occur deeper in the soil profile than implied if varying CO₂ production is explained entirely by a
616 Q₁₀ mechanism. Ishikura *et al.* (2018) invoked physical transport processes to explain their
617 observation of flux oscillations peaking at night. Oscillating temperature may drive advective
618 and diffusive fluxes from the peat surface through a variety of mechanisms. As the peat warms,
619 soil gas expands, driving a gas flux from the peat surface. The maximum shallow temperature
620 swing at the sunny location drives an expansion of the gas volume in the near-surface peat by
621 about 12%, 7% from thermal expansion of gas and 5% from evaporation of water. As the peat
622 heats, this gas expansion can increase flux by both pushing CO₂ from the peat and increasing the
623 gradient driving CO₂ diffusion from the peat; when the peat cools at night, both processes
624 reverse, cooling gas contracts and water vapor condenses. To a lesser degree, shifts in the
625 solubility of CO₂ and diffusion coefficients with temperature will also increase daytime and
626 decrease nighttime fluxes from the peat surface. Determining the importance of these physical
627 processes in the diurnal pattern of flux measured at the peat surface, and the interactions of these
628 processes, would require a detailed numerical model of gas behavior in the peat column that is
629 beyond the scope of this paper. Here, we point out that such physical processes may create daily
630 oscillations in flux independent of decomposition processes.

631

632 **D) Limitations**

633
634
635
636
637
638
639
640
641
642
643
644
645
646
647
648
649
650
651

Despite the strong trends we observe, we recognize a number of methodological limitations to our chamber-based approach. The chamber and collar design inherently modify local conditions. In particular, the root exclusion method may greatly affect decomposition processes, as soil moisture, temperature, and carbon and nutrient cycling are disrupted by the absence of roots. Thus measurements of R_{het} in root-cut conditions may differ substantially from rates of R_{het} in undisturbed conditions (reviewed in Kuzyakov, 2006, 2010), although some evidence suggests that enhancement or inhibition of decomposition by roots may be limited in highly organic soils (Linkosalmi *et al.*, 2015). Additionally, the tall collar design could affect air flow. Due to the dense understory of regenerating vegetation and remnant small trees, wind movement near the surface is usually limited at the site, but localized convective transport could play a more important role and may be affected by the tall collar design (Ishikura *et al.*, 2018a). Shrinkage of the peat near collars could also modify local gas transport, though there was no visible evidence of gaps near collars. Finally, flux and peat temperature measurements were made over two consecutive but non-overlapping time periods. Although simultaneous measurements of both variables would give more precise results, qualitative findings would most likely be similar because both time periods included a similar range of water table depths and diurnal oscillation in temperature and CO_2 flux were highly regular.

652 **E) Conclusions and Implications for Further Work**

653
654
655
656
657
658
659
660
661

In summary, we find CO_2 flux is strongly dependent on water table depth over days to months (A), and has a pronounced diurnal oscillation which follows peat temperature at hourly timescales (B). A satisfactory model for heterotrophic respiration in peat must account for both observations A and B (Figure 5). We explored three mechanisms that could help account for both the increase in average emissions at low water tables and the diurnal oscillation in fluxes: (i) the nonlinear effect of temperature on respiration (Q_{10}); (ii) decreased soil moisture in surface peat at low water tables; and (iii) temperature-dependent transport of soil gas.

662
663

Of these three mechanisms, (i) the nonlinear relationship between temperature and decomposition is insufficient to explain the observed data. However, (ii) physical transport

664 mechanisms, and (iii) increased near-surface decomposition due to changes in soil moisture
665 remain plausible. Both mechanisms emphasize the important indirect control of water table depth
666 on heterotrophic respiration. A mix of these two mechanisms is likely, although we are unable to
667 quantify their role here. To conclusively resolve this issue would require detailed depth profile
668 measurements of CO₂, combined with a model to disentangle the effects of CO₂ transport and
669 production.

670
671 Our observations also have important practical implications. The strong diurnal cycle in
672 CO₂ flux suggests that if manual chamber measurements are limited to midday, they may
673 significantly overestimate mean daily fluxes under some conditions, particularly in open
674 degraded peatlands. This highlights the importance of making hourly measurements, and/or
675 determining correction factors to less frequent measurements. Finally, our upscaling of both
676 carbon export as DOC and R_{het} based on water table time series suggests that drainage will
677 continue to be the most important driver of CO₂ fluxes from tropical peatlands in the region.
678 These findings show that hourly measurements are an important foundation for quantification of
679 the carbon budget of tropical peatlands.

680

681 **Acknowledgements**

682

683 We thank Mahmud Yussof of Brunei Darussalam Heart of Borneo Center and the Brunei
684 Darussalam Ministry of Industry and Primary Resources for their support of this project; Hajah
685 Jamilah Jalil and Joffre Ali Ahmad of the Brunei Darussalam Forestry Department
686 for facilitation of field work and release of staff; Amy Chua for project support; Bernard Jun
687 Long Ng, Jefferey Muli Anak Incham, Ramasamy Anak Zulkiflee, and Haji Bohari Bin Haji Idi
688 for field assistance; and Lucy Hutyra for technical guidance. This research was supported by the
689 National Research Foundation Singapore through the Singapore–MIT Alliance for Research and
690 Technology’s Center for Environmental Sensing and Modeling interdisciplinary research
691 program, by the US National Science Foundation under Grants 1114155 and 1114161 (to
692 C.F.H.), and by a grant from the Environmental Solutions Initiative at Massachusetts Institute of
693 Technology.

694

695 **References**

696

697 Ali M, Taylor D, Inubushi K (2006) Effects of environmental variations on CO₂ efflux from a tropical
698 peatland in Eastern Sumatra. *Wetlands*, **26**, 612–618.

699 Blackham G V, Thomas A, Webb EL, Corlett RT (2013) Seed rain into a degraded tropical peatland in
700 Central Kalimantan, Indonesia. *Biological Conservation*, **167**, 215–223.

701 Brady MA (1997) *Organic Matter Dynamics of Coastal Peat Deposits in Sumatra, Indonesia*. PhD thesis,
702 The University of British Columbia.

703 Carlson KM, Goodman LK, May-Tobin CC (2015) Modeling relationships between water table depth and
704 peat soil carbon loss in Southeast Asian plantations. *Environmental Research Letters*, **10**, 074006.

705 Cobb AR, Hoyt AM, Gandois L, Eri J, Dommain R, Salim KA, Kai FM, Su'ut NSH, Harvey CF (2017)
706 How temporal patterns in rainfall determine the geomorphology and carbon fluxes of tropical
707 peatlands. *Proceedings of the National Academy of Sciences*, **114**, E5187–E5196.

708 Comeau L-P, Hergoualc'h K, Hartill J, Smith J, Verchot L V, Peak D, Salim AM (2016) How do the
709 heterotrophic and the total soil respiration of an oil palm plantation on peat respond to nitrogen
710 fertilizer application? *Geoderma*, **268**, 41–51.

711 Couwenberg J, Dommain RR, Joosten H (2010) Greenhouse gas fluxes from tropical peatlands in south-
712 east Asia. *Global Change Biology*, **16**, 1715–1732.

713 Cussler EL (1997) *Diffusion: Mass Transfer in Fluid Systems*, 2nd Editio edn. Cambridge University
714 Press, New York, 45078 pp.

715 Davidson EA, Janssens IA (2006) Temperature sensitivity of soil carbon decomposition and feedbacks to
716 climate change. *Nature*, **440**, 165–173.

717 Davidson EA, Janssens IA, Luo Y (2006) On the variability of respiration in terrestrial ecosystems:
718 moving beyond Q₁₀. *Global Change Biology*, **12**, 154–164.

719 Dommain R, Couwenberg J, Glaser PH, Joosten H, Suryadiputra INN (2014) Carbon storage and release
720 in Indonesian peatlands since the last deglaciation. *Quaternary Science Reviews*, **97**, 1–32.

721 Dommain R, Cobb AR, Joosten H et al. (2015) Forest dynamics and tip-up pools drive pulses of high

- 722 carbon accumulation rates in a tropical peat dome in Borneo (Southeast Asia). *Journal of*
723 *Geophysical Research: Biogeosciences*, **120**, 617–640.
- 724 Fang C, Moncrieff JB (2001) The dependence of soil CO₂ efflux on temperature. *Soil Biology and*
725 *Biochemistry*, **33**, 155–165.
- 726 Gandois L, Cobb AR, Hei IC, Lim LBL, Salim KA, Harvey CF (2013) Impact of deforestation on solid
727 and dissolved organic matter characteristics of tropical peat forests: implications for carbon release.
728 *Biogeochemistry*, **114**, 183–199.
- 729 Gandois L, Teisserenc R, Cobb AR et al. (2014) Origin, composition, and transformation of dissolved
730 organic matter in tropical peatlands. *Geochimica et Cosmochimica Acta*, **137**, 35–47.
- 731 Gastaldo RA (2010) Peat or no peat: Why do the Rajang and Mahakam Deltas differ? *International*
732 *Journal of Coal Geology*, **83**, 162–172.
- 733 Gharedaghlou B, Price JS, Rezanezhad F, Quinton WL (2018) Evaluating the hydraulic and transport
734 properties of peat soil using pore network modeling and X-ray micro computed tomography.
735 *Journal of Hydrology*, **561**, 494–508.
- 736 Heinemeyer A, McNamara NP (2011) Comparing the closed static versus the closed dynamic chamber
737 flux methodology: Implications for soil respiration studies. *Plant Soil*, **346**, 145–151.
- 738 Hergoualc'h K, Hendry DT, Murdiyarso D, Verchot LV (2017) Total and heterotrophic soil respiration in
739 a swamp forest and oil palm plantations on peat in Central Kalimantan, Indonesia. *Biogeochemistry*,
740 **135**, 203–220.
- 741 Hirano T, Jauhiainen J, Inoue T, Takahashi H (2009) Controls on the carbon balance of tropical peatlands.
742 *Ecosystems*, **12**, 873–887.
- 743 Hirano T, Kusin K, Limin S, Osaki M (2014) Carbon dioxide emissions through oxidative peat
744 decomposition on a burnt tropical peatland. *Global Change Biology*, **20**, 555–565.
- 745 Hooijer A, Page S, Canadell JG, Silvius M, Kwadijk J, Wösten H, Jauhiainen J (2010) Current and future
746 CO₂ emissions from drained peatlands in Southeast Asia. *Biogeosciences*, **7**, 1505–1514.
- 747 Hooijer A, Page S, Jauhiainen J, Lee WA, Lu XX, Idris A, Anshari G (2012) Subsidence and carbon loss
748 in drained tropical peatlands. *Biogeosciences*, **9**, 1053–1071.
- 749 Husnain H, Wigena IGP, Dariah A, Marwanto S, Setyanto P, Agus F (2014) CO₂ emissions from tropical

- 750 drained peat in Sumatra, Indonesia. *Mitigation and Adaptation Strategies for Global Change*, **19**,
751 845–862.
- 752 Ishikura K, Hirano T, Okimoto Y et al. (2018a) Soil carbon dioxide emissions due to oxidative peat
753 decomposition in an oil palm plantation on tropical peat. *Agriculture, Ecosystems and Environment*,
754 **254**, 202–212.
- 755 Ishikura K, Darung U, Inoue T, Hatano R (2018b) Variation in soil properties regulate greenhouse gas
756 fluxes and global warming potential in three land use types on tropical peat. *Atmosphere*, **9**, 1–14.
- 757 Jauhiainen J, Limin S, Silvennoinen H, Vasander H (2008) Carbon dioxide and methane fluxes in drained
758 tropical peat before and after hydrological restoration. *Ecology*, **89**, 3503–3514.
- 759 Jauhiainen J, Hooijer A, Page SE (2012) Carbon dioxide emissions from an *Acacia* plantation on peatland
760 in Sumatra, Indonesia. *Biogeosciences*, **9**, 617–630.
- 761 Jauhiainen J, Kerojoki O, Silvennoinen H, Limin S, Vasander H (2014) Heterotrophic respiration in
762 drained tropical peat is greatly affected by temperature—a passive ecosystem cooling experiment.
763 *Environmental Research Letters*, **9**, 105013.
- 764 Jauhiainen J, Silvennoinen H, Könönen M, Limin S, Vasander H (2016) Management driven changes in
765 carbon mineralization dynamics of tropical peat. *Biogeochemistry*, **129**, 115–132.
- 766 Kobayashi S (1999) Initial phase of secondary succession in the exploited peat swamp forest (*Shorea*
767 *albida*) at Sungai Damit, Belait in Brunei Darussalam. In: *Proceedings of the International*
768 *Symposium on Tropical Peatlands (ISTP)*, pp. 205–214. Bogor.
- 769 Kottek M, Grieser J, Beck C, Rudolf B, Rubel F (2006) World Map of the Köppen-Geiger climate
770 classification updated. **15**, 259–263.
- 771 Kutzbach L, Schneider J, Sachs T et al. (2007) CO₂ flux determination by closed-chamber methods can
772 be seriously biased by inappropriate application of linear regression. *Biogeosciences*, **4**, 1005–1025.
- 773 Kuzyakov Y (2006) Sources of CO₂ efflux from soil and review of partitioning methods. *Soil Biology and*
774 *Biochemistry*, **38**, 425–448.
- 775 Kuzyakov Y (2010) Priming effects: Interactions between living and dead organic matter. *Soil Biology*
776 *and Biochemistry*, **42**, 1363–1371.
- 777 LI-COR (2010) LI-8100A Automated Soil CO₂ Flux System & LI-8150 Multiplexer Instruction Manual.

- 778 Linkosalmi M, Pumpanen J, Biasi C et al. (2015) Studying the impact of living roots on the
779 decomposition of soil organic matter in two different forestry-drained peatlands. *Plant Soil*, **396**,
780 59–72.
- 781 Livingston GP, Hutchinson GL, Spartalian K (2005) Diffusion theory improves chamber-based
782 measurements of trace gas emissions. **32**, L24817.
- 783 Lloyd J, Taylor JA (1994) On the temperature dependence of soil respiration. *Functional Ecology*, **8**,
784 315–323.
- 785 Marwanto S, Agus F (2014) Is CO₂ flux from oil palm plantations on peatland controlled by soil moisture
786 and/or soil and air temperatures? *Mitigation and Adaptation Strategies for Global Change*, **19**, 809–
787 819.
- 788 Melling L, Hatano R, Goh KJ (2005) Soil CO₂ flux from three ecosystems in tropical peatland of Sarawak
789 , Malaysia. *Tellus*, **57B**, 1–11.
- 790 Miettinen J, Shi C, Liew SC (2016) Land cover distribution in the peatlands of Peninsular Malaysia,
791 Sumatra and Borneo in 2015 with changes since 1990. *Global Ecology and Conservation*, **6**, 67–78.
- 792 Miettinen J, Hooijer A, Vernimmen R, Liew SC, Page SE (2017) From carbon sink to carbon source:
793 extensive peat oxidation in insular Southeast Asia since 1990. *Environmental Research Letters*, **12**,
794 024014.
- 795 Moyano FE, Manzoni S, Chenu C (2013) Responses of soil heterotrophic respiration to moisture
796 availability: An exploration of processes and models. *Soil Biology and Biochemistry*, **59**, 72–85.
- 797 Murayama S, Bakar ZA (1996a) Decomposition of tropical peat soils: 1. Decomposition kinetics of
798 organic matter of peat soils. *Japan Agricultural Research Quarterly*, **30**, 145–151.
- 799 Murayama S, Bakar ZA (1996b) Decomposition of tropical peat soils: 2. Estimation of in-situ
800 decomposition by measurement of CO₂ flux. *Japan Agricultural Research Quarterly*, **30**, 153–158.
- 801 NOAA (2019) Cold & warm episodes by season, Oceanic Niño Index. *National Centers for*
802 *Environmental Prediction*, 8–10.
- 803 Page SE, Rieley JO, Banks CJ (2011a) Global and regional importance of the tropical peatland carbon
804 pool. *Global Change Biology*, **17**, 798–818.
- 805 Page SE, Morrison R, Malins C, Hooijer A, Rieley JO, Jauhiainen J (2011b) *Review of Peat Surface*

807 Rezanezhad F, Quinton W, Price J, Elliot T, Elrick D, Shook K (2010) Influence of pore size and
 808 geometry on peat unsaturated hydraulic conductivity computed from 3D computed tomography
 809 image analysis. *Hydrological Processes*, **24**, 2983–2994.

810 Tuomi M, Vanhala P, Karhu K, Fritze H, Liski J (2008) Heterotrophic soil respiration-Comparison of
 811 different models describing its temperature dependence. *Ecological Modelling*, **211**, 182–190.

812 Wickland KP, Neff JC (2008) Decomposition of soil organic matter from boreal black spruce forest:
 813 Environmental and chemical controls. *Biogeochemistry*, **87**, 29–47.

814 Wright EL, Black CR, Cheesman AW, Drage T, Large D, Turner BL, Sjögersten S (2011) Contribution
 815 of subsurface peat to CO₂ and CH₄ fluxes in a neotropical peatland. *Global Change Biology*, **17**,
 816 2867–2881.

817 **Tables:**

818

819

Timing	Measurements Conducted
Period 1: Jul 2012 – Nov 2012	<ul style="list-style-type: none"> • CO₂ Flux: Sun • CO₂ Flux: Shade • Water table and precipitation • Air temperature
Period 2: Nov 2013 – Mar 2014	<ul style="list-style-type: none"> • Peat temperature: Sun • Peat temperature: Shade • Air temperature • Water table at the nearby Mendaram peatland (2012-2015)

820

821 **Table 1. Timeline of measurements.** Measurements were conducted over two study periods. CO₂ Flux
 822 measurements were conducted during the first period. Peat temperature was measured during the second
 823 study period.

824

825 **Figure Captions:**

826

827 **Figure 1. Chamber Locations.** (a) Sunny chamber (chamber 1). (b-d) Shaded chambers (chambers 2, 3
828 & 4 respectively) (e) Schematic of chamber layout. Circles indicate chamber locations (C1-C4), the
829 triangle indicates the location of ground water measurements (GWL), the small square indicates the
830 location of the infrared gas analyzer (IRGA), the large square indicates the solar power supply and the
831 star indicates a large remnant *Shorea albida* tree (SA). Precipitation was measured on the roof of the solar
832 power supply. (f) Map of insular Southeast Asia with peatland area (grey) and study site in Brunei
833 Darussalam (black star) indicated.

834

835

836 **Figure 2. CO₂ Flux and Water Table Measurements.** (a) CO₂ flux (R_{het}) vs water table depth. Colored
837 dots represent hourly measurements at each individual chamber. Large black circles represent the daily
838 mean across all chambers. Data from August-November shown. The y-axis is truncated for clarity, so the
839 highest hourly measurements do not appear. (b) Timeseries of individual chamber hourly measurements
840 of CO₂ efflux (colored) and daily mean values (black). (c) Time series of water table depth over study
841 period 1, covering the typical range of conditions experienced at this nondrained site. (d) Time series inset
842 shows diurnal cycle over the course of a week. Daytime peaks are largest in the sun (Chamber 1).

843

844 **Figure 3. Upscaling CO₂ and DOC Fluxes.** (a) Time series of calculated mean daily heterotrophic
845 respiration (R_{het}) from hollows (dark grey), R_{het} from across the peat dome (light grey; calculated using a
846 topographic offset of 4.8cm), and DOC export. Y-axis truncates peak DOC export of 46 μ mol/m²/s in Mar
847 2012. (b) Fitted carbon loss by heterotrophic respiration (R_{het}) from hollows ($R^2 = 0.92$), calculated R_{het}
848 from across the peat dome, calculated DOC export, and measured daily mean CO₂ flux vs. water table
849 depth are shown on the right axis (truncated for visibility). A histogram of water table depth at the site is
850 shown on the left axis. The water table spends most of the time near the surface where both DOC export
851 and CO₂ emissions are small, perhaps facilitating peat stability. (c) Measured time series of water table
852 depth from Feb 6, 2012-Feb 6, 2015 from the nearby undrained Mendaram peatland used for upscaling.

853

854 **Figure 4. Diurnal Cycle.** (a & b) R_{het} flux vs time of day. Hourly measurements are aggregated for water
855 table depth ranges for sun and shaded chambers. (c, d, e & f): Hourly measurements of peat temperature
856 at different depths in the soil for sun, shade, wet and dry conditions. Largest diurnal oscillations are seen

857 under dry conditions in the sun. Wet/dry cutoff is 5cm below the peat surface (Figure S2). g) Hourly air
858 temperature averaged across days. Oscillations are greatest under dry conditions. h) Air temperature
859 maximum, mean and minimum vs. water table depth.

860

861

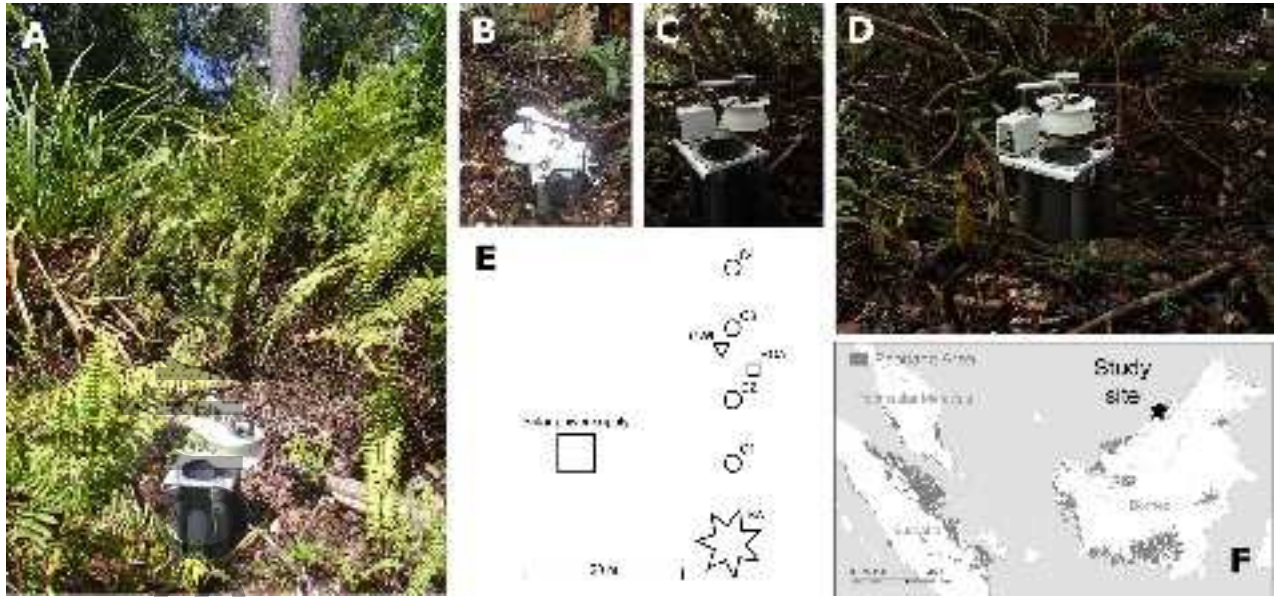
862 **Figure 5. Hourly measurements as a percentage of daily mean for (a) sun and (b) shade.** Daytime
863 measurements have the potential to significantly overestimate daily mean fluxes, particularly in the sun,
864 and under relatively dry conditions.

865

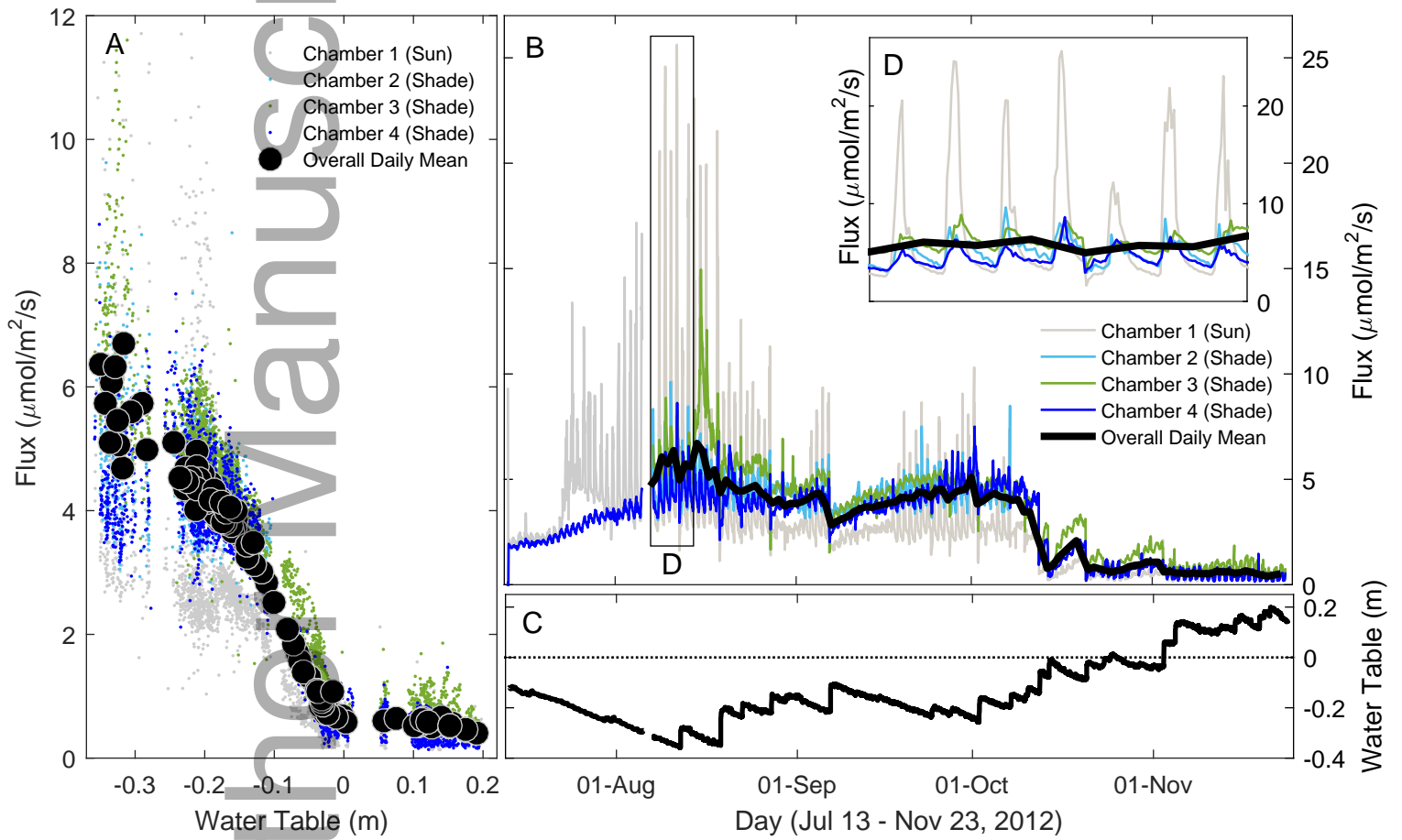
866

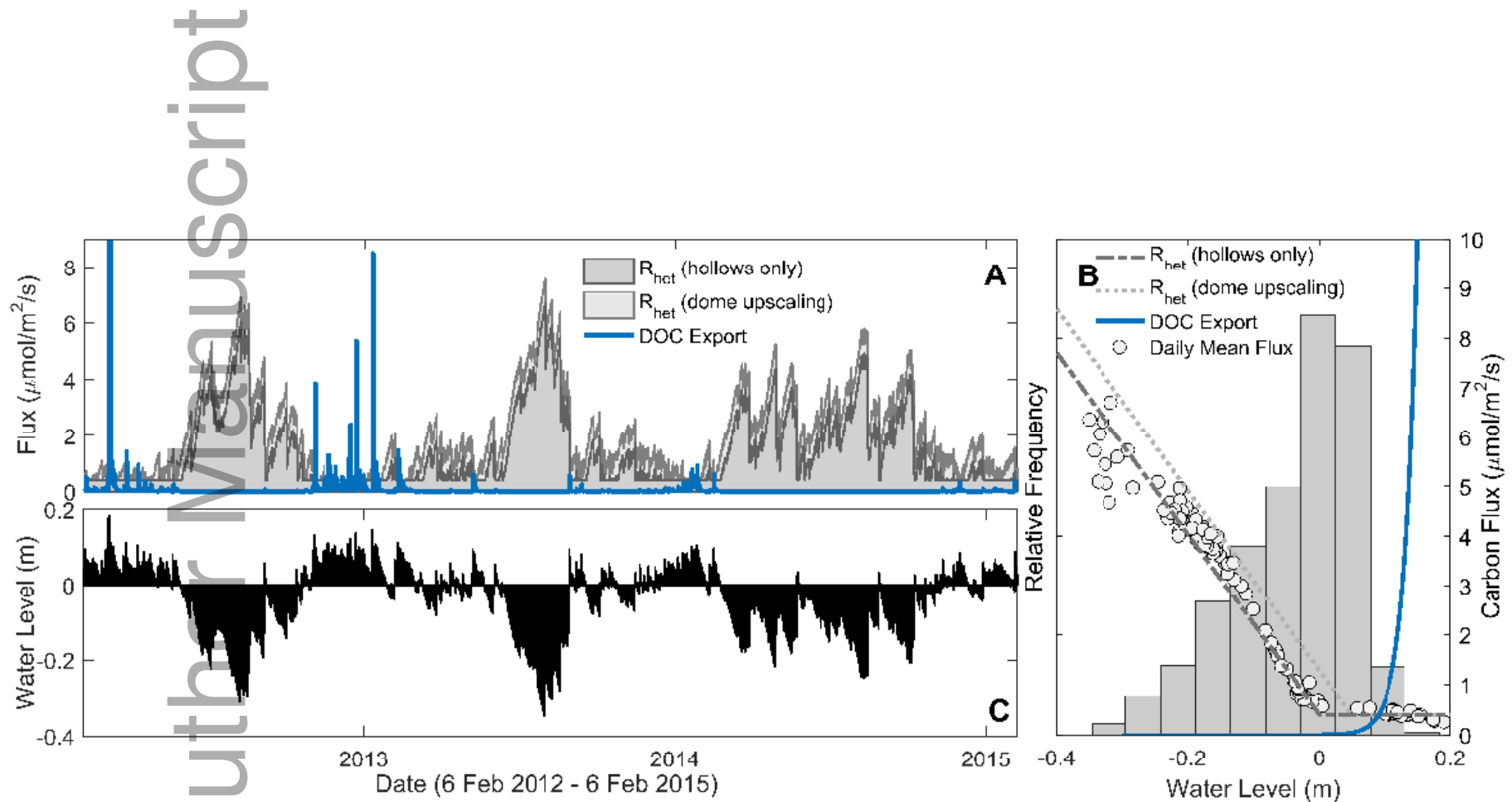
867 **Figure 6. Explaining key observations from chamber measurements in tropical peatlands.** The
868 relationship between mean daily CO₂ flux and water table depth explored in section A could be simply
869 explained by uniform CO₂ production through the peat profile above the water table. The diurnal
870 oscillations in CO₂ flux discussed in section B could be simply (but incompatibly) explained if CO₂
871 production is dominated by near-surface decomposition. Section C explores mechanisms that could
872 account for both observations A and B.

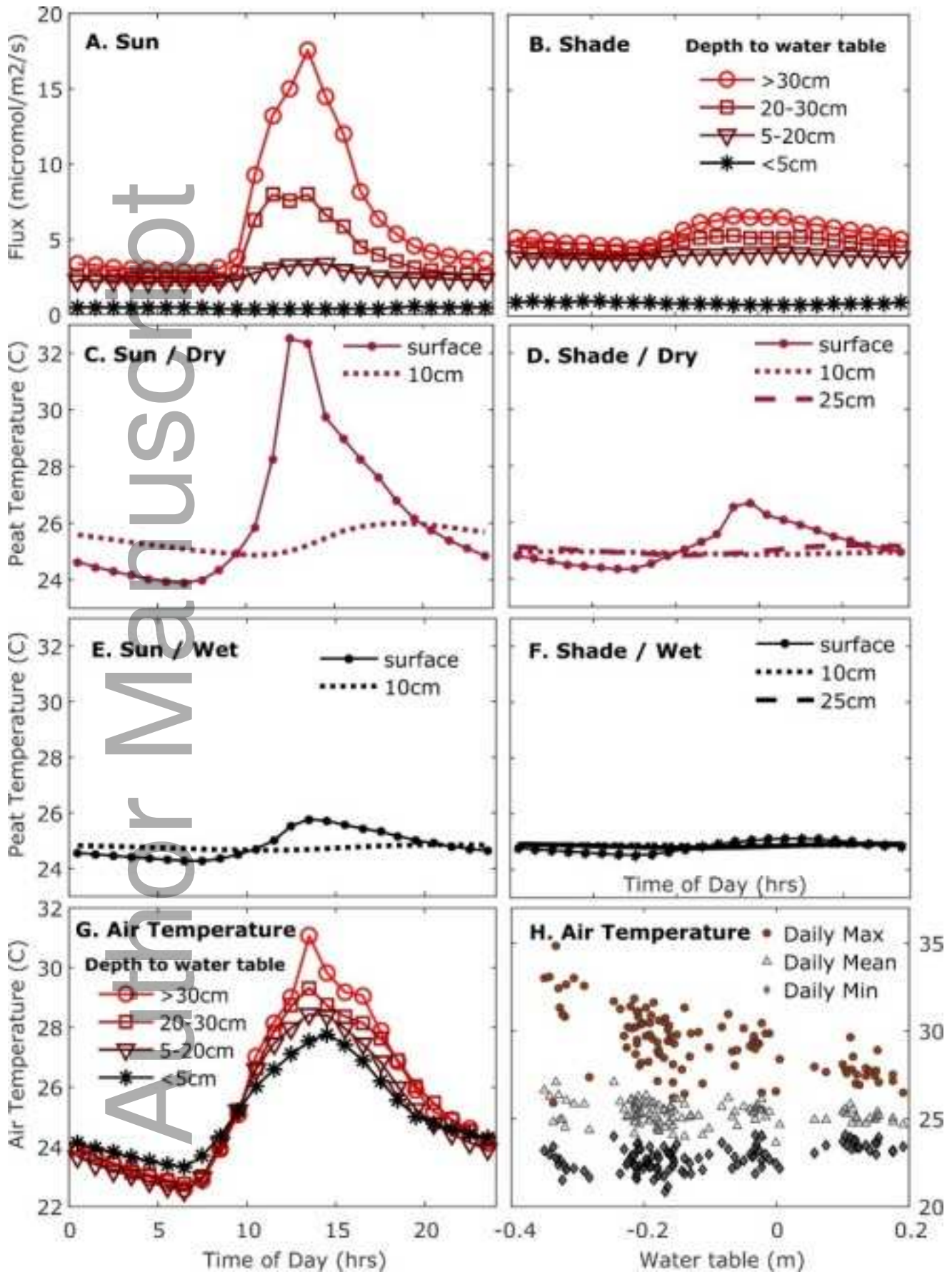
Author Manuscript



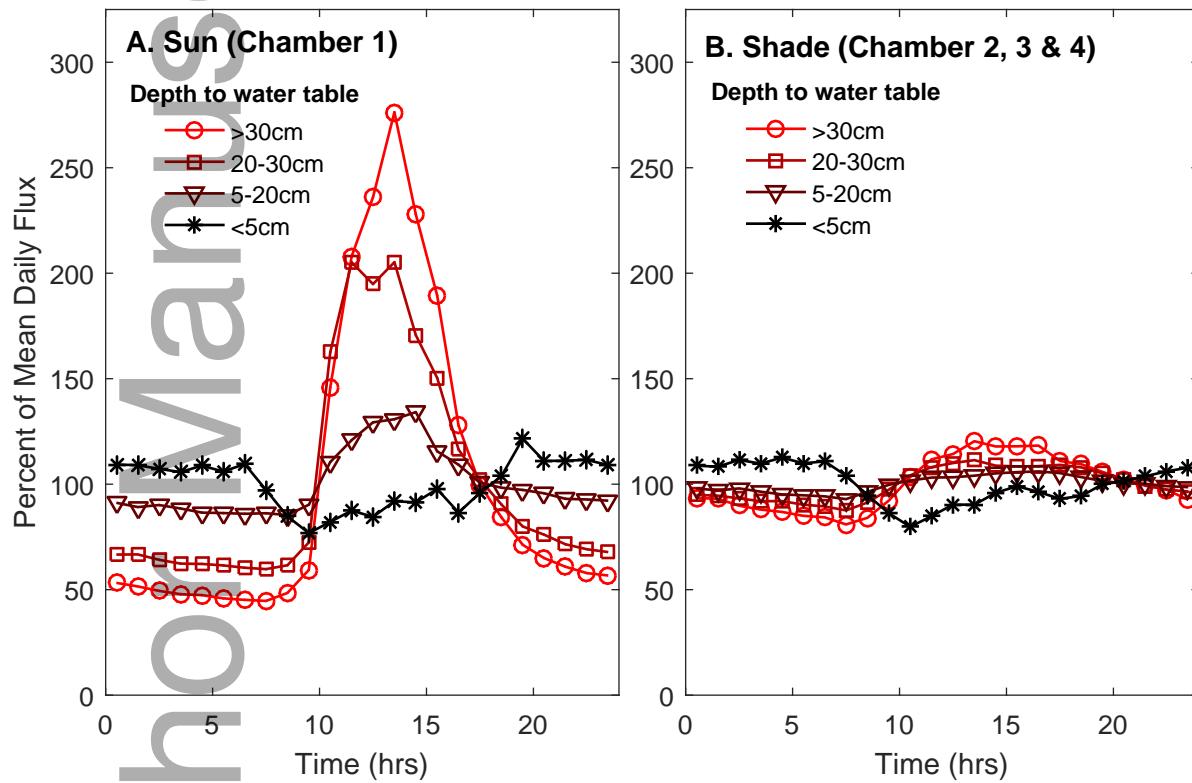
gcb_14702_f1.png







gcb_14702_f4.png



Author Manuscript

	A	Observations:	B
Key Observation	Mean daily CO ₂ flux is proportional to aerobic zone thickness		CO ₂ flux and peat temperature follow synchronous oscillations
Timescale	Daily		Hourly
Simple Model:			
Dominant Control	Water table depth		Temperature
Depth of CO ₂ Production	Uniform decomposition through oxic peat profile		Decomposition of shallow peat dominates
Inconsistency	Fails to explain daily oscillations		Fails to explain WTD dependency
C Possible Mechanisms Consistent with A & B:			
<ul style="list-style-type: none"> (i) Oscillating temperature drives nonlinear R_{het} (ii) Variations in moisture control R_{het} (iii) Temperature dependent transport processes affect CO₂ flux 			